


**ORIGINAL ARTICLE**

# Regulation of capillary hemodynamics by $K_{ATP}$ channels in resting skeletal muscle

Daniel M. Hirai<sup>1,2</sup>  | Ayaka Tabuchi<sup>2,3</sup> | Jesse C. Craig<sup>2,4,5</sup> | Trenton D. Colburn<sup>2</sup> | Timothy I. Musch<sup>2,6</sup> | David C. Poole<sup>2,6</sup>

<sup>1</sup>Department of Health and Kinesiology, Purdue University, West Lafayette, Indiana, USA

<sup>2</sup>Department of Kinesiology, Kansas State University, Manhattan, Kansas, USA

<sup>3</sup>Department of Engineering Science, University of Electro-Communications, Tokyo, Japan

<sup>4</sup>Department of Internal Medicine, University of Utah, Salt Lake City, Utah, USA

<sup>5</sup>Geriatric Research, Education and Clinical Center, Veterans Affairs Medical Center, Salt Lake City, Utah, USA

<sup>6</sup>Department of Anatomy and Physiology, Kansas State University, Manhattan, Kansas, USA

**Correspondence**

Daniel M. Hirai, Department of Health and Kinesiology, College of Health and Human Sciences, Purdue University, 800 W. Stadium Ave., Lambert 201C, West Lafayette, IN, USA.  
Email: dhirai@purdue.edu

**Funding information**

This work was supported in part by a Post-Doctoral Fellowship from the College of Human Ecology, Kansas State University; PRF Summer Faculty Grant, Purdue University; and National Heart, Lung and Blood Institute Grant HL-2-108328.

**Abstract**

ATP-sensitive  $K^+$  channels ( $K_{ATP}$ ) have been implicated in the regulation of resting vascular smooth muscle membrane potential and tone. However, whether  $K_{ATP}$  channels modulate skeletal muscle microvascular hemodynamics at the capillary level (the primary site for blood-myocyte  $O_2$  exchange) remains unknown. We tested the hypothesis that  $K_{ATP}$  channel inhibition would reduce the proportion of capillaries supporting continuous red blood cell (RBC) flow and impair RBC hemodynamics and distribution in perfused capillaries within resting skeletal muscle. RBC flux ( $f_{RBC}$ ), velocity ( $V_{RBC}$ ), and capillary tube hematocrit ( $Hct_{cap}$ ) were assessed via intravital microscopy of the rat spinotrapezius muscle ( $n = 6$ ) under control (CON) and glibenclamide (GLI;  $K_{ATP}$  channel antagonist; 10  $\mu M$ ) superfusion conditions. There were no differences in mean arterial pressure (CON:  $120 \pm 5$ , GLI:  $124 \pm 5$  mmHg;  $p > 0.05$ ) or heart rate (CON:  $322 \pm 32$ , GLI:  $337 \pm 33$  beats/min;  $p > 0.05$ ) between conditions. The %RBC-flowing capillaries were not altered between conditions (CON:  $87 \pm 2$ , GLI:  $85 \pm 1\%$ ;  $p > 0.05$ ). In RBC-perfused capillaries, GLI reduced  $f_{RBC}$  (CON:  $20.1 \pm 1.8$ , GLI:  $14.6 \pm 1.3$  cells/s;  $p < 0.05$ ) and  $V_{RBC}$  (CON:  $240 \pm 17$ , GLI:  $182 \pm 17$   $\mu m/s$ ;  $p < 0.05$ ) but not  $Hct_{cap}$  (CON:  $0.26 \pm 0.01$ , GLI:  $0.26 \pm 0.01$ ;  $p > 0.05$ ). The absence of GLI effects on the %RBC-flowing capillaries and  $Hct_{cap}$  indicates preserved muscle  $O_2$  diffusing capacity ( $DO_{2m}$ ). In contrast, GLI lowered both  $f_{RBC}$  and  $V_{RBC}$  thus impairing perfusive microvascular  $O_2$  transport ( $Q_m$ ) and lengthening RBC capillary transit times, respectively. Given the interdependence between diffusive and perfusive  $O_2$  conductances (i.e., % $O_2$  extraction  $\propto DO_{2m}/Q_m$ ), such GLI alterations are expected to elevate muscle % $O_2$  extraction to sustain a given metabolic rate. These results support that  $K_{ATP}$  channels regulate capillary hemodynamics and, therefore, microvascular gas exchange in resting skeletal muscle.

**KEYWORDS**

ATP-sensitive  $K^+$  channel, blood flow, intravital microscopy, microcirculation, red blood cell

## 1 | INTRODUCTION

The skeletal muscle capillary vascular bed provides the largest surface area for gas and substrate exchange within the body (Hirai et al., 2019; Poole et al., 2011; Poole, 2019). Regulation of skeletal muscle capillary hemodynamics is mediated primarily at the arteriolar level (Joyner & Casey, 2015; Kindig & Poole, 2001; Laughlin et al., 2012; Segal, 2005). Several complex and often interacting mechanisms are responsible for alterations in arteriolar resistance and thus vascular conductance. Among these processes,  $K^+$  channels constitute the dominant ion conductance of the vascular smooth muscle cell determining membrane potential, contractile activity, and thus vascular tone (Foster & Coetzee, 2016; Jackson, 2017; Tykocki et al., 2017).

ATP-sensitive  $K^+$  ( $K_{ATP}$ ) channels constitute one of the, at least, five distinct classes of  $K^+$  channels regulating vascular smooth muscle function (Foster & Coetzee, 2016; Jackson, 2017; Tykocki et al., 2017). Inhibition (closing) of  $K_{ATP}$  channels decreases  $K^+$  efflux leading to depolarization of the smooth muscle cell. Voltage-gated  $Ca^{2+}$  channels then transduce membrane depolarization into increased  $Ca^{2+}$  influx promoting vascular muscle contraction (i.e., vasoconstriction). *In vitro* and *in vivo* studies have thus used pharmacological  $K_{ATP}$  channel inhibition to evaluate its potential role in setting vascular tone and, consequently, tissue perfusion. Sulfonylureas such as glibenclamide (GLI), which are employed clinically in the treatment of non-insulin-dependent diabetes (Montvida et al., 2018), represent the most frequently used class of  $K_{ATP}$  channel inhibitors. To date, however, there is a lack of agreement regarding the role of  $K_{ATP}$  channels in the regulation of resting vascular tone and blood flow within skeletal muscle (Foster & Coetzee, 2016; Jackson, 2017; Tykocki et al., 2017).  $K_{ATP}$  channel inhibition with GLI has produced conflicting effects on resting skeletal muscle arteriolar diameter (Hammer et al., 2001; Hodnett et al., 2008; Jackson, 1993; Lu et al., 2013; Murrant & Sarelius, 2002; Saito et al., 1996; Xiang & Hester, 2009) and bulk blood flow (Bank et al., 2000; Colburn, Holdsworth, et al., 2020; Duncker et al., 2001; Farouque & Meredith, 2003a,b; Holdsworth et al., 2015; Vanelli & Hussain, 1994). Importantly, the functional role of  $K_{ATP}$  channels within the skeletal muscle capillary network (i.e., the primary site for blood-myocyte  $O_2$  exchange) remains to be determined. Resolution of the mechanisms modulating capillary red blood cell (RBC) hemodynamics has direct relevance to transcapillary  $O_2$  flux and cellular energetic status.

The purpose of this study was to evaluate the regulation of capillary RBC hemodynamics by  $K_{ATP}$  channels in resting skeletal muscle. Using intravital microscopy techniques combined with the rat spinotrapezius preparation, we tested the hypothesis that acute local  $K_{ATP}$  channel inhibition with GLI would impair key determinants of capillary diffusive and

perfusible  $O_2$  conductances. Specifically, GLI was anticipated to reduce the proportion of capillaries supporting continuous RBC flow and impair microvascular hemodynamics and distribution (i.e., RBC flux, velocity, and capillary tube hematocrit) in perfused capillaries within resting skeletal muscle. Confirmation of these hypotheses would support a role for  $K_{ATP}$  channels in the regulation of skeletal muscle capillary hemodynamics (and thus microvascular gas exchange) under resting conditions.

## 2 | METHODS

Intravital microscopy was used to evaluate the *in vivo* spinotrapezius muscle microcirculation in healthy young male Sprague–Dawley rats ( $n = 6$ ; ~3–4 months old;  $386 \pm 26$  g). Rats were maintained in accredited facilities (Association for the Assessment and Accreditation of Laboratory and Animal Care) under a 12:12 h light–dark cycle with food and water provided *ad libitum*. All experimental procedures and protocols were approved by the Institutional Animal Care and Use Committee of Kansas State University and followed the guidelines established by the National Institutes of Health.

### 2.1 | Surgical procedures

#### 2.1.1 | Anesthesia and catheter placement procedures

All rats were anesthetized initially with a 5% isoflurane- $O_2$  mixture and maintained subsequently on 2–3% isoflurane- $O_2$  (Butler Animal Health Supply). Anesthetized rats were kept on a heating pad to maintain core temperature at ~37–38°C as measured via a rectal probe. The right carotid artery was cannulated (PE-10 connected to PE-50; BD IntraMedic Polyethylene Tubing) for continuous measurements of mean arterial pressure and heart rate (MAP and HR, respectively; PowerLab; ADInstruments). The caudal artery was cannulated (PE-10 connected to PE-50) for infusion of anesthetic agents. Isoflurane inhalation was then discontinued progressively and rats were kept under anesthesia with pentobarbital sodium (50 mg/kg i.a.) throughout the remainder of the experiment. Anesthesia level was monitored at frequent and regular intervals via the toe-pinch and blink reflexes and supplemented as necessary (0.02–0.05 ml of 50 mg/ml pentobarbital sodium diluted in ~0.2 ml of heparinized saline).

#### 2.1.2 | Intravital microscopy preparation

The rat spinotrapezius muscle was used for the microcirculatory studies herein because a) its exteriorization

allows for clear visualization of capillary structure and hemodynamics via light transmission microscopy (Gray, 1973; Poole et al., 1997); b) it can be exteriorized without neural or substantial vascular disruption (Bailey et al., 2000; Gray, 1973; Poole et al., 1997); c) a physiological sarcomere length can be maintained throughout the experimental protocol (thereby preventing muscle overstretching and adverse microcirculatory effects) (Poole et al., 1997; Welsh & Segal, 1996); and d) its mixed fiber-type composition and oxidative capacity are similar to those of the human quadriceps (Delp & Duan, 1996; Leek et al., 2001), thus representing a useful analog of human locomotor muscle. Following catheter placement procedures, the left spinotrapezius was exposed and exteriorized as described previously (Bailey et al., 2000; Gray, 1973; Poole et al., 1997) with minimal fascial removal to limit tissue damage and microcirculatory disturbances (Mazzoni et al., 1990). Briefly, the caudal end of the muscle was isolated from its origin and sutured at equidistant points to a horseshoe-shaped manifold. The rat was then placed on a water circulation-heated (38°C) Lucite platform and the manifold secured with the ventral aspect of the muscle reflected upwards for microscopic observation. The preparation was frequently superfused with Krebs–Henseleit bicarbonate-buffered solution (2.0 mM CaCl<sub>2</sub>, 2.4 mM MgSO<sub>4</sub>, 4.7 mM KCl, 22 mM NaHCO<sub>3</sub>, 131 mM NaCl; pH 7.4; equilibrated with 5% CO<sub>2</sub> and 95% N<sub>2</sub> at ~38°C) and exposed surrounding tissue covered with Saran wrap (Dow Brands). As noted earlier, the spinotrapezius was maintained at physiological sarcomere length (2.6 ± 0.1 μm) to prevent stretch-induced reductions in capillary blood flow (Poole et al., 1997; Welsh & Segal, 1996).

## 2.2 | Experimental protocol

### 2.2.1 | Intravital video microscopy

Microcirculatory fields located midway between arteriolar and venular ends within the mid-caudal region of the spinotrapezius that provided optimal clarity were selected randomly for the study. Microcirculatory images were obtained via a bright-field microscope (Nikon Eclipse E600-FN) equipped with a non-contact illuminated lens (x40, numerical aperture 0.8) and viewed in real time on a high-resolution color monitor (Sony Trinitron PVM-1954Q) under a final magnification of x1,184 (as confirmed by initial calibration of the system with a stage micrometer; MA285; Meiji Techno). Images were recorded by a video camera (JVC KY-F55B) and stored on a computer for subsequent offline analyses.

### 2.2.2 | Experimental design

Once the spinotrapezius muscle was positioned on the platform, a quiescent period of at least 15 min was allowed before any data were acquired. Intravital microscopy recordings were then made under two separate superfusion conditions: control (Krebs–Henseleit; CON) and K<sub>ATP</sub> channel inhibition (glibenclamide; GLI). GLI was the last treatment due to its long-lasting effects (Thomas et al., 1997) and the possibility of incomplete washout with Krebs–Henseleit. All superfusion solutions were maintained at approximately 38°C. The spinotrapezius was superfused with each solution for 3 min (average flow rate of 1 ml/min) followed by a 30 min equilibration period as employed by previous microcirculatory studies (Hodnett et al., 2008; Jackson, 1993; Lu et al., 2013; Murrant & Sarelius, 2002; Saito et al., 1996). Microcirculatory fields were chosen randomly from each rat (based on clear visualization of sarcomeres, fibers, and capillaries) and each recorded for ~1–1.5 min. At the end of the experimental protocol, rats were killed with intra-arterial pentobarbital sodium overdose (100 mg/kg) followed by pneumothorax.

### 2.2.3 | Acute local K<sub>ATP</sub> channel inhibition

The pharmacological sulphonylurea derivative GLI (494 g/mol; 5-chloro-*N*-[4-(cyclohexylureidosulfonyl)phenethyl]-2-methoxybenzamide; Sigma-Aldrich; St. Louis, MO) was used to inhibit K<sub>ATP</sub> channels via superfusion (topical application) of the spinotrapezius muscle. GLI stock solutions were made fresh daily with the solvent dimethyl sulfoxide (DMSO) and diluted with control (Krebs–Henseleit) superfusate. The final working superfusate had a GLI concentration of 10 μM and contained <0.01% DMSO. This GLI concentration was based on previous microcirculatory research using similar drug delivery methods with the rat spinotrapezius and hamster cheek pouch and cremaster muscles (Cohen & Sarelius, 2002; Hammer et al., 2001; Hodnett et al., 2008; Jackson, 1993; Lu et al., 2013; Murrant & Sarelius, 2002; Saito et al., 1996; Xiang & Hester, 2009). Previous studies have shown that ≤0.05% DMSO solutions have no significant effects on resting skeletal muscle arteriolar diameter or reactivity (Cohen et al., 2000; Jackson, 1993) or K<sub>ATP</sub> channel currents in the absence or presence of ATP (Mele et al., 2014; Tricarico et al., 2006). Recent reports from our laboratory have shown no differences in arterial blood PO<sub>2</sub>, PCO<sub>2</sub>, O<sub>2</sub> saturation, hematocrit, pH, [lactate] or [glucose] following superfusion of the rat spinotrapezius muscle with K<sub>ATP</sub> channel agonists (pinacidil; 5 mg/kg) and antagonists (GLI; 5 mg/kg) (Holdsworth et al., 2017).

## 2.3 | Analysis of muscle capillary hemodynamics

Within each preparation, only those microcirculatory fields with the best overall clarity were selected for further examination via frame-by-frame techniques (30 frames/s; Dartfish) as described previously (Kindig et al., 1999, 2002; Poole et al., 1997). Sarcomere length was determined from sets of 10 consecutive in-register sarcomeres (i.e., distance between 11 consecutive A-bands) measured in parallel to the muscle fiber longitudinal axis. This procedure was repeated 3 times where sarcomeres were visible to obtain a mean sarcomere length for each field. Comparisons between control and GLI conditions were made within the same microcirculatory field for each rat and, whenever possible, between the same capillaries (which occurred in ~47% of cases; i.e., 14 of 30 vessels). The percentage of RBC-perfused vessels was established as (no. of capillaries supporting RBC flow/total no. of visible capillaries per field)  $\times$  100. Vessels demonstrating impeded or stopped flow (i.e., stationary or no visible RBC flow) for  $\geq 10$  s were regarded as non-flowing capillaries. Five capillaries supporting continuous RBC flow were selected randomly for hemodynamics analysis from each microcirculatory field based on clarity. For all capillaries in which hemodynamics was evaluated and where the capillary endothelium was clearly visible on both sides of the lumen, capillary luminal diameter ( $d_{\text{cap}}$ ) was measured at two random sites per capillary (2–3 measurements/site). RBC velocity ( $V_{\text{RBC}}$ ) was determined by following the RBC path length over several frames and for the maximum capillary length over which the cells remained in crisp focus. RBC flux ( $f_{\text{RBC}}$ ) was measured by counting the number of cells in a capillary passing an arbitrary point over several frames. These measurements were performed three times per capillary. For each capillary in which hemodynamics data were measured, capillary tube hematocrit ( $\text{Hct}_{\text{cap}}$ ) was calculated as follows:

$$\text{Hct}_{\text{cap}} = (\text{vol}_{\text{RBC}} \times f_{\text{RBC}}) / [\pi \times (d_{\text{cap}}/2)^2 \times V_{\text{RBC}}] \quad (1)$$

where  $\text{vol}_{\text{RBC}}$  is RBC volume and assumed to be  $61 \mu\text{m}^3$  (Altman & Dittmer, 1974) and capillaries were approximated as circular in cross section (Desjardins & Duling, 1990; Kindig et al., 1998).

## 2.4 | Statistical analyses

Statistical analyses were performed using a commercially available software package (SigmaPlot 11.2; Systat Software). Data distribution was assessed via the Shapiro–Wilk test for normality. Central hemodynamics (MAP and HR) and spinotrapezius muscle capillary structure ( $d_{\text{cap}}$ ) and hemodynamics (%RBC-flowing capillaries,  $f_{\text{RBC}}$ ,  $V_{\text{RBC}}$ , and

$\text{Hct}_{\text{cap}}$ ) data were compared between control and GLI conditions using paired Student's *t*-tests. Coefficients of variation were calculated as (SD/mean)  $\times$  100 and compared between control and GLI conditions using the methods described by Forkman (2009). Pearson's product-moment correlations and linear regression analyses were used to examine relationships between  $f_{\text{RBC}}$  and  $V_{\text{RBC}}$ . Linear regression slope comparisons were performed as described by Zar (1984). Significance was accepted at  $p < 0.05$ . Data are reported as mean  $\pm$  SE.

## 3 | RESULTS

### 3.1 | Central hemodynamics

As expected based on the topical drug delivery method employed herein (i.e., local superfusion of the spinotrapezius muscle), no differences in MAP (CON:  $120 \pm 5$ , GLI:  $124 \pm 5$  mmHg;  $p > 0.05$ ) or HR (CON:  $322 \pm 32$ , GLI:  $337 \pm 33$  beats/min;  $p > 0.05$ ) were observed between conditions.

### 3.2 | Spinotrapezius muscle capillary structure and hemodynamics

The percentage of capillaries supporting continuous RBC flow was not altered between conditions (Figure 1;  $p > 0.05$ ). Capillaries subjected to hemodynamics analysis supported RBC flow prior to, and continued to do so, following  $\text{K}_{\text{ATP}}$

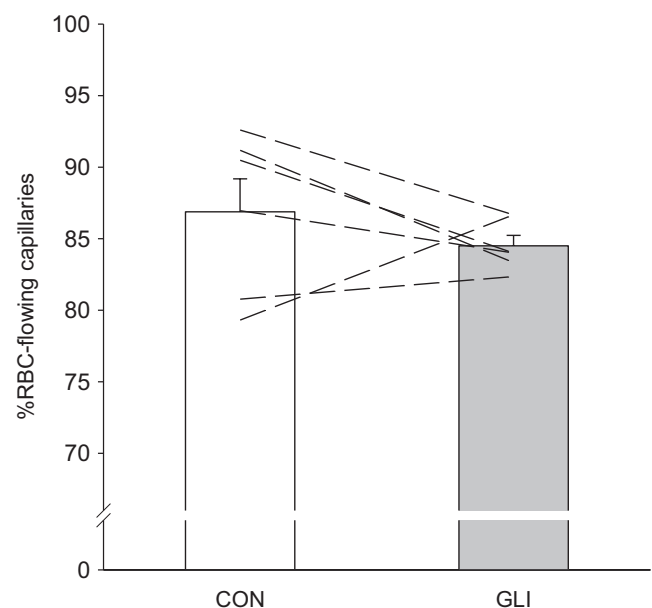


**FIGURE 1** Percentage of capillaries supporting red blood cell (RBC) flow during control (CON;  $n = 6$ ) and  $\text{K}_{\text{ATP}}$  channel inhibition (glibenclamide, GLI;  $n = 6$ ) conditions. Dashed lines represent individual muscle data

inhibition (i.e., during CON and GLI, respectively). In these RBC-flowing capillaries, GLI reduced both  $f_{\text{RBC}}$  and  $V_{\text{RBC}}$  (Figures 2 and 3;  $p < 0.05$  for both) but not  $\text{Hct}_{\text{cap}}$  (CON:  $0.26 \pm 0.01$ , GLI:  $0.26 \pm 0.01$ ;  $p > 0.05$ ). GLI-induced alterations in muscle capillary hemodynamics occurred in the absence of changes in  $d_{\text{cap}}$  between conditions (CON:  $4.9 \pm 0.1$ , GLI:  $4.9 \pm 0.1 \mu\text{m}$ ;  $p > 0.05$ ). Frequency histograms of capillary  $f_{\text{RBC}}$  and  $V_{\text{RBC}}$  are shown in Figure 3. Microvascular blood flow heterogeneity, as evaluated by the individual capillary coefficient of variation, was not different

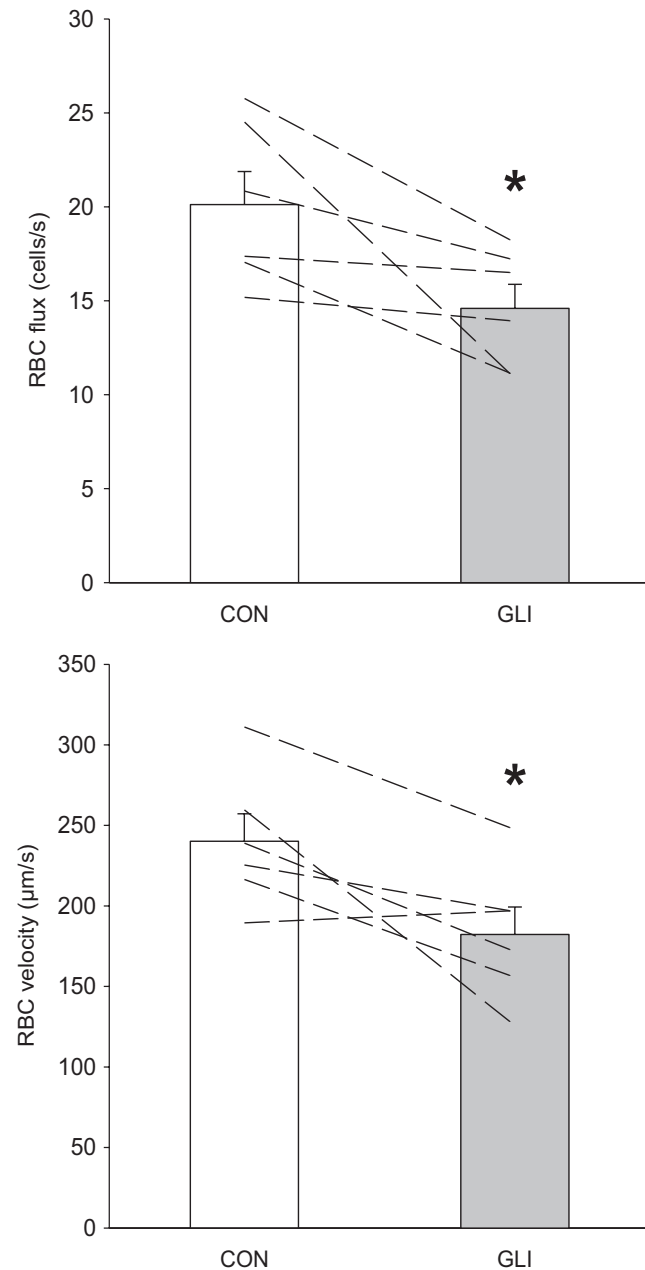


**FIGURE 2** Capillary red blood cell flux (top panel) and velocity (bottom panel) during control (CON;  $n = 6$ ) and  $\text{K}_{\text{ATP}}$  channel inhibition (glibenclamide, GLI;  $n = 6$ ) conditions. Dashed lines represent individual muscle data. \* $p < 0.05$  vs. CON

between conditions with respect to  $f_{\text{RBC}}$  (CON: 61.8, GLI: 57.4%;  $p > 0.05$ ),  $V_{\text{RBC}}$  (CON: 49.4, GLI: 47.8%;  $p > 0.05$ ) or  $\text{Hct}_{\text{cap}}$  (CON: 23.6, GLI: 22.3%;  $p > 0.05$ ). Similar results were found when comparing heterogeneity between microvascular fields in terms of  $f_{\text{RBC}}$  (CON: 21.4, GLI: 21.6%;  $p > 0.05$ ),  $V_{\text{RBC}}$  (CON: 17.4, GLI: 22.9%;  $p > 0.05$ ), and  $\text{Hct}_{\text{cap}}$  (CON: 13.5, GLI: 11.1%;  $p > 0.05$ ).

Consistent with the lack of changes in  $\text{Hct}_{\text{cap}}$  with GLI (and the relationship described in Eq. 1 above), no significant differences were observed in the slope of the  $f_{\text{RBC}}/V_{\text{RBC}}$  relationship between conditions (individual capillaries; CON: 8.75, GLI: 9.44; individual muscles; CON: 7.46, GLI: 12.25;  $p > 0.05$  for both). Therefore, Figure 4 presents linear correlations and regression analyses for the combined CON and GLI data. Capillary  $f_{\text{RBC}}$  and  $V_{\text{RBC}}$  were significantly correlated

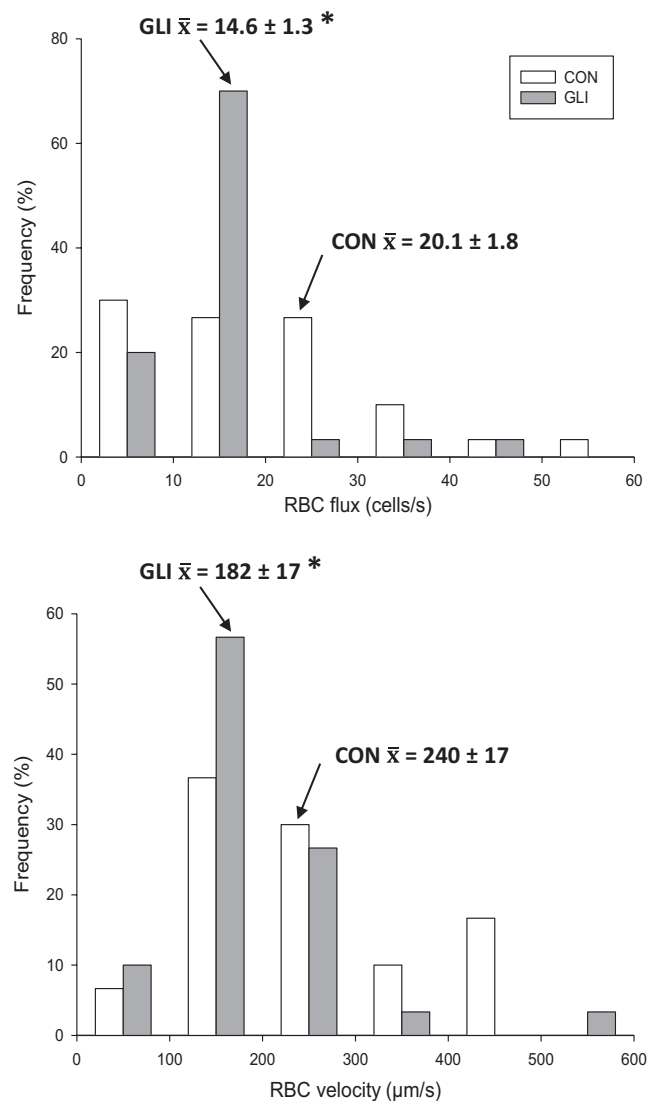


**FIGURE 3** Relative frequency histograms of capillary red blood cell flux (top panel) and velocity (bottom panel) during control (CON;  $n = 6$ ) and  $\text{K}_{\text{ATP}}$  channel inhibition (glibenclamide, GLI;  $n = 6$ ) conditions. Arrows show mean values. \* $p < 0.05$  vs. CON



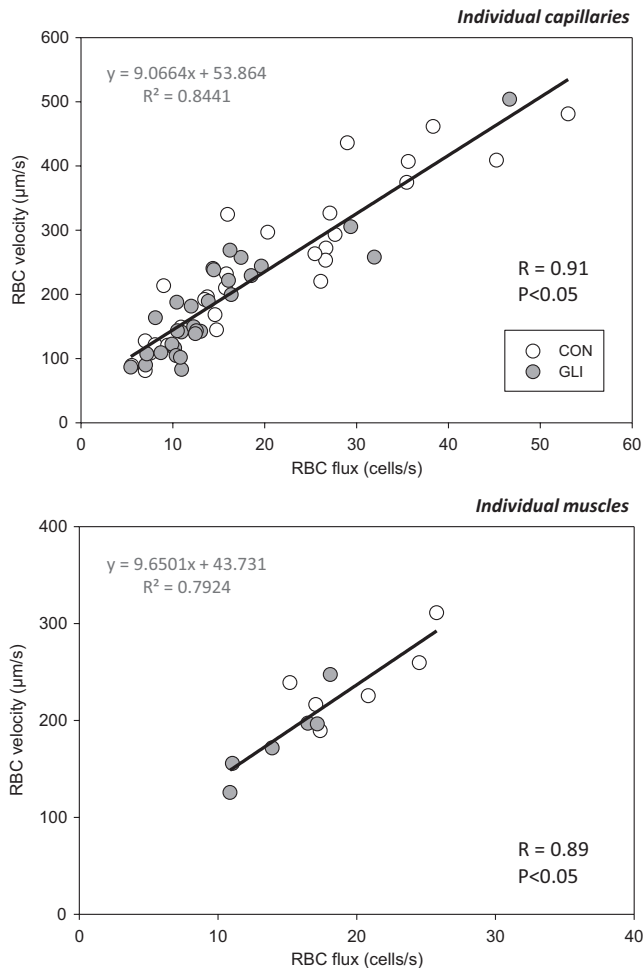


**FIGURE 4** Individual and mean capillary relationships (*top* and *bottom* panels, respectively) between red blood cell flux and velocity during control (CON) and  $K_{ATP}$  channel inhibition (glibenclamide, GLI) conditions. Each data point represents a single capillary in the *top* panel ( $n = 30$ ) and the average value for all capillaries within a single muscle ( $n = 6$ ) in the *bottom* panel

in both individual capillaries and individual muscles (Figure 4, *top* and *bottom* panels, respectively) thus illustrating their proportional reduction with GLI.

## 4 | DISCUSSION

This investigation examined, for the first time, the regulation of capillary hemodynamics by  $K_{ATP}$  channels in resting skeletal muscle. Superfusion of the rat spinotrapezius with the sulfonyleurea GLI was used to locally inhibit  $K_{ATP}$  channels *in vivo*. The principal novel findings are as follows: a) inconsistent with our hypothesis, GLI did not reduce the proportion of capillaries supporting continuous RBC flow or  $Hct_{cap}$ ; and b) consistent with our hypothesis, GLI lowered microvascular blood flow (i.e., both  $f_{RBC}$  and  $V_{RBC}$ ) in perfused capillaries. These data suggest that  $K_{ATP}$  channels,

via modulation of arteriolar vascular conductance, regulate microvascular hemodynamics at the capillary level (the primary site for blood-myocyte  $O_2$  diffusion) (Hirai et al., 2019; Poole et al., 2011; Poole, 2019) in resting skeletal muscle.

### 4.1 | Intravital microscopy preparation

Surgical exteriorization of the rat spinotrapezius muscle was performed as described previously (Bailey et al., 2000; Gray, 1973; Poole et al., 1997) with minimal fascial disturbance to curtail tissue damage and related microcirculatory consequences. Accordingly, previous studies from our laboratory indicate that the surgical exteriorization requisite for transmission intravital microscopy as performed herein does not impair the microvascular integrity or responsiveness of the spinotrapezius muscle (Bailey et al., 2000).

In the present investigation, spinotrapezius sarcomere length was set at physiological values ( $2.6 \pm 0.1 \mu\text{m}$ ) to prevent stretch-induced capillary luminal diameter reductions (Poole et al., 1997) and/or sympathetically mediated decreases in arteriolar blood flow (Welsh & Segal, 1996; cf. Kindig & Poole, 2001). Capillary structure ( $d_{cap}$ ) and hemodynamics ( $\%RBC$ -flowing vessels,  $f_{RBC}$ ,  $V_{RBC}$ , and  $Hct_{cap}$ ) data obtained herein during the control condition are consistent with those published previously in the resting rat spinotrapezius and hamster cheek pouch and cremaster muscles (Copp et al., 2009; Kano et al., 2005; Kindig et al., 1998, 1999, 2002; Kindig & Poole, 2001; Poole et al., 1997; Richardson et al., 2003; Russell et al., 2003; Sarelius & Duling, 1982). Our data are also consistent with the well-documented lower than systemic  $Hct_{cap}$  values found in resting skeletal muscle (Poole et al., 2011; Poole, 2019). Based on both theoretical and empirical studies, potential mechanisms for the systemic versus capillary tube hematocrit difference include a) the presence of the endothelial surface layer (i.e., the often termed “glycocalyx”); b) the Fahraeus effect; and c) plasma skimming at arteriolar bifurcations (Desjardins & Duling, 1990; Ellsworth et al., 2009; Pries et al., 1986; Secomb et al., 1998).

As reviewed recently (Poole et al., 2011; Poole, 2019), a compelling body of evidence demonstrates that the vast majority of skeletal muscle capillaries support continuous RBC perfusion at rest. Our data are consistent with this notion showing that  $\sim 85\%$  of capillaries supported continuous  $f_{RBC}$  during both CON and GLI conditions (Figure 1).

### 4.2 | Local $K_{ATP}$ channel inhibition with GLI superfusion

As expected, GLI-induced alterations in microvascular hemodynamics ( $f_{RBC}$  and  $V_{RBC}$ ; Figure 2) occurred in the absence of changes in  $d_{cap}$  between conditions. This suggests

increased vascular resistance at sites upstream of the capillary bed consistent with the well-established arteriolar control of skeletal muscle blood flow (Joyner & Casey, 2015; Kindig & Poole, 2001; Laughlin et al., 2012; Segal, 2005). Our data are thus in agreement with some, but not all, reports of decreased arteriolar diameter (Hammer et al., 2001; Hodnett et al., 2008; Jackson, 1993; Lu et al., 2013; Murrant & Sarelius, 2002; Saito et al., 1996; Xiang & Hester, 2009) and bulk blood flow (Bank et al., 2000; Colburn, Weber, et al., 2020; Duncker et al., 2001; Farouque & Meredith, 2003a,b; Holdsworth et al., 2015; Vanelli & Hussain, 1994) following  $K_{ATP}$  channel inhibition in the resting skeletal muscle. Potential reasons for this discrepancy include species differences, experimental models, GLI doses,  $K_{ATP}$  channel density distribution, compensatory vasodilation by redundant pathways, muscle fiber type, and arteriolar size and branch order. Although providing an invaluable framework for understanding the control of vascular tone and tissue perfusion, previous measurements of arteriolar diameter and bulk blood flow responses with GLI presented no information concerning the distribution of microvascular flow within the capillary network. Moreover, it was not known whether  $K_{ATP}$  channel inhibition would impact uniformly RBC-perfused capillaries or whether the proportion of RBC-perfused capillaries could be reduced. Evaluation of capillary hemodynamics within those vessels supporting continuous RBC flow is critical to identifying how  $K_{ATP}$  channels may modulate blood-myocyte  $O_2$  and substrate exchange. This is especially true when considering that the capillary network provides the largest surface area for gas and substrate exchange within the skeletal muscle microcirculation (Hirai et al., 2019; Poole et al., 2011; Poole, 2019).

The potential for  $K_{ATP}$  channels to modulate skeletal muscle  $O_2$  exchange must be considered in light of the interdependence between diffusive and perfusive conductances setting fractional  $O_2$  extraction (Roca et al., 1992):

$$\% O_2 \text{ extraction} = 1 - e^{-DO_{2m}/\beta Q_m} \quad (2)$$

where  $DO_{2m}$  is muscle  $O_2$  diffusing capacity,  $\beta$  is the slope of the  $O_2$  dissociation curve in the physiologically relevant range, and  $Q_m$  is muscle blood flow. Theoretical models of skeletal muscle  $O_2$  exchange indicate that  $DO_{2m}$  is determined by structural (capillary-to-fiber ratio, capillary length, and  $d_{cap}$ ) and functional ( $Hct_{cap}$  at constant arterial  $O_2$  saturation) elements (Federspiel & Popel, 1986; Groebe & Thews, 1990). Capillary-to-fiber ratio, capillary length, and  $\beta$  are not expected to be affected by acute GLI treatment as employed herein. Moreover, we observed no differences in  $d_{cap}$  or  $Hct_{cap}$  between CON and GLI. It thus seems that  $K_{ATP}$  channels do not modulate significantly  $DO_{2m}$  in resting skeletal muscle. On the other hand, the current GLI-induced reductions in  $f_{RBC}$  (which largely dictates  $Q_m$  within the microcirculation) (Berg & Sarelius, 1996) are

anticipated to elevate the  $DO_{2m}/Q_m$  ratio within RBC-perfused capillaries and, therefore, necessitate higher muscle fractional  $O_2$  extraction for a given metabolic rate according to Eq. 2 above. Importantly, the functional consequence of lowered  $f_{RBC}$  with GLI (Figure 2, *top panel*) is impaired  $O_2$  delivery per capillary ( $QO_{2cap}$ ). Disregarding the small amount of  $O_2$  dissolved in plasma (and, therefore, its relevance to capillary gas exchange),  $QO_{2cap}$  can be estimated as the product of  $f_{RBC}$ , the hemoglobin content per RBC ( $17 \times 10^{-12}$  g per RBC) (Altman & Dittmer, 1974) and the  $O_2$  carrying capacity of hemoglobin (at 89% saturation, assuming arterial  $PO_2 = 80$  mmHg in anesthetized rats) as described previously (Kindig et al., 1998):

$$\dot{Q}O_{2cap} = f_{RBC} (\text{g Hb} \times \text{RBC}^{-1}) (1.34 \text{ ml } O_2 \times \text{g Hb}^{-1} \times 0.89) \quad (3)$$

Using the equation above,  $K_{ATP}$  inhibition with GLI superfusion of the resting spinotrapezius herein reduced mean  $QO_{2cap}$  by approximately 27% from 4.08 to  $2.96 \times 10^{-10}$  ml  $O_2/s$ . Interestingly, this estimation is strikingly similar to the ~28% reduction in total hindlimb skeletal muscle blood flow of conscious resting rats following GLI administration (Colburn, Holdsworth, et al., 2020).

GLI-induced alterations in  $V_{RBC}$  (Figure 2, *bottom panel*) underscore the potential of  $K_{ATP}$  channels to further modulate capillary gas exchange via changes in RBC transit time. Given the ~25% decrease in  $V_{RBC}$  with GLI observed herein and the mean capillary length within the rat spinotrapezius (i.e., 430  $\mu\text{m}$  based on previous morphometric analyses by Gray, 1984), total capillary RBC residence time is calculated to increase from ~1.8 s during control to ~2.4 s following  $K_{ATP}$  channel inhibition. While it is acknowledged that these calculations may underestimate true residence time due to the actual RBC path length being somewhat longer than the anatomical path length (Sarelius, 1986), the amount of error introduced should not preferentially bias either superfusion condition. Longer RBC transit times provide the mechanistic basis for the elevated fractional  $O_2$  extraction expected with GLI as discussed above.

The proportional reductions in  $f_{RBC}$  and  $V_{RBC}$  with GLI were such that  $Hct_{cap}$  remained unchanged between conditions (*vide supra* its mathematical description; Eq. 1). It is interesting that the relationship between  $f_{RBC}$  and  $V_{RBC}$  in the resting skeletal muscle may also be preserved with aging and some disease states. Accordingly, previous studies from our laboratory have shown that the microvascular dysregulation characteristic of aging (Copp et al., 2009; Russell et al., 2003), type I diabetes (Kindig et al., 1998), and chronic heart failure (Kindig et al., 1999; Richardson et al., 2003) does not appear to affect resting  $Hct_{cap}$ . As noted above,  $Hct_{cap}$  is a primary determinant of  $DO_{2m}$  and, therefore, diffusive  $O_2$  conductance within the microcirculation (Federspiel & Popel, 1986; Groebe & Thews, 1990). This derives from the low  $O_2$  diffusivity in plasma and the particulate nature of blood,

which render only the capillary surface area in close proximity to the RBC functional for diffusion at any given time. The current  $Hct_{cap}$  data thus indicate preserved capillary surface area available for diffusive  $O_2$  exchange within continuously RBC-perfused vessels following  $K_{ATP}$  channel inhibition.

An important question for future studies is whether the impairments in resting capillary hemodynamics seen here after  $K_{ATP}$  inhibition are also present during muscle contractions and, if so, their potential implications for exercise tolerance. In the resting spinotrapezius, GLI lowered  $f_{RBC}$  and  $V_{RBC}$  (i.e., reduced  $Q_m$ ; Figure 2) whilst not affecting  $Hct_{cap}$  or the %RBC-flowing capillaries (i.e., unaltered  $DO_{2m}$  as noted above), thereby predisposing to higher fractional  $O_2$  extraction (i.e., higher  $DO_{2m}/Q_m$  ratio; Eq. 2). While there has been no prior evaluation of  $K_{ATP}$  channel inhibition on contracting muscle capillary blood flow *per se*, studies on arteriolar diameter and bulk blood flow have produced contrasting evidence regarding the role of  $K_{ATP}$  channels in functional hyperemia (Tykocki et al., 2017). Nonetheless, recent reports from our laboratory indicate that GLI lowers microvascular  $O_2$  partial pressures ( $PO_2$ ) as well as estimated  $DO_{2m}$  in the contracting spinotrapezius and mixed gastrocnemius muscles (Colburn, Weber, et al., 2020; Holdsworth et al., 2016). Under these circumstances, intramyocyte  $PO_2$  is expected to fall to generate the driving pressure ( $\Delta PO_2$ ) and possibly elevate intramyocyte  $O_2$  diffusing capacity by and by further deoxygenating myoglobin as necessary to maintain a given metabolic rate as described by Fick's law of diffusion:

$$\dot{V}O_2 = DO_{2m} \times \Delta PO_2 \quad (4)$$

where  $\dot{V}O_2$  corresponds to the rate of  $O_2$  flux,  $DO_{2m}$  is the diffusing capacity as defined above and  $\Delta PO_2$  the  $O_2$  partial pressure difference between the microvascular and intramyocyte spaces. Reduction in intramyocyte  $PO_2$  can be problematic because it promotes depletion of finite muscle phosphocreatine and glycogen stores, intracellular accumulation of metabolites (including ADP, Pi, and  $H^+$ ) and acid-base perturbations associated with fatigue (Hogan et al., 1992; Wilson et al., 1977). Therefore, based on the above observations, potential impairments in contracting muscle capillary hemodynamics with GLI could result in pernicious consequences for oxidative metabolism and exercise tolerance (Colburn, Weber, et al., 2020; Lu et al., 2013).

Despite marked reductions in RBC hemodynamics (i.e., decreased  $f_{RBC}$  and  $V_{RBC}$ ; Figure 2), GLI did not change microvascular blood flow heterogeneity (as evaluated by the coefficient of variation of  $f_{RBC}$ ,  $V_{RBC}$ , and  $Hct_{cap}$ ) in the resting spinotrapezius. Due to the nature of our experimental protocol (i.e., assessment of the same microcirculatory fields, and whenever possible, capillaries between conditions), these data indicate that any spatial vascular/metabolic mismatch present at rest was not exacerbated with GLI. Whether the

same holds true for the contracting skeletal muscle (amid dynamic temporal and spatial changes in  $O_2$  delivery-utilization) remains to be determined. Importantly, the consequences of microvascular blood flow heterogeneity assume greater significance during exercise when high  $O_2$  fluxes (which can rise >100-fold compared to rest) are required to support oxidative metabolism.

### 4.3 | Clinical implications

Sulfonylureas are the most popular second-line treatment prescribed for type 2 diabetes mellitus (Montvida et al., 2018), promoting insulin release via inhibition of pancreatic  $K_{ATP}$  channels. However, systemic inhibition of  $K_{ATP}$  channels with these oral medications may also compromise key components of capillary gas exchange within skeletal muscle as revealed herein (i.e., lowered  $f_{RBC}$  and  $V_{RBC}$ ; Figure 2). The latter microvascular impairments compound with those described previously in the diabetic skeletal muscle (Kindig et al., 1998; Padilla et al., 2006) thus questioning the therapeutic value of sulfonylurea medications for diabetic patients. Systemic sulfonylurea administration has also been reported to reduce contracting muscle bulk blood flow (Holdsworth et al., 2015; Keller et al., 2004; Thomas et al., 1997) and submaximal and maximal exercise tolerance (Colburn, Weber, et al., 2020; Lu et al., 2013). Although no decrements in intracapillary  $DO_{2m}$  with GLI were found herein at rest, potential reductions in the proportion of capillaries supporting continuous RBC flow with sulfonylurea medications during contractions would be expected to impair muscle glucose uptake (via reductions in exchange surface area). As such, exercise intolerance may be exacerbated in diabetes by systemic sulfonylurea medications impairing  $K_{ATP}$  channel regulation of skeletal muscle capillary hemodynamics.

### 4.4 | Experimental considerations

Superfusion of the spinotrapezius muscle with GLI was employed herein to locally inhibit  $K_{ATP}$  channels *in vivo*. This topical drug delivery method was chosen to prevent the potential confound of alterations in central hemodynamics (e.g., MAP, HR, systemic vascular resistance), myocardial hemodynamics and function (e.g., coronary vascular conductance and  $O_2$  delivery, left ventricular relaxation rate), sympathetic nerve activity, visceral organ blood flow, blood insulin and glucose concentration, among others with systemic drug administration as reported previously (Colburn, Holdsworth, et al., 2020; Colburn, Weber, et al., 2020; Duncker et al., 2001; Farouque & Meredith, 2003a; Holdsworth et al., 2015, 2016; Rocha et al., 2020; Thomas et al., 1997). Nonetheless, it is not possible to pinpoint the



site of GLI action (e.g., across the vascular network and/or among distinct cell types) with the current experimental protocol. Although our GLI concentration and superfusion protocol were based on previous microcirculatory studies (Cohen & Sarelius, 2002; Hammer et al., 2001; Hodnett et al., 2008; Jackson, 1993; Lu et al., 2013; Murrant & Sarelius, 2002; Saito et al., 1996; Xiang & Hester, 2009) as described earlier, this approach could lead to non-specific vasodilation (Jiang et al., 2007; Tykocki et al., 2017) and potentially underestimate the contribution of  $K_{ATP}$  channels to microvascular control. It is noteworthy that, despite the latter considerations and the modest sample size ( $n = 6$ ), significant GLI-induced reductions in  $f_{RBC}$  and  $V_{RBC}$  were observed in the resting spinotrapezius muscle (Figures 2 and 3). Post hoc power calculations indicate that a total of 48 animals would be needed to detect significant changes in the %RBC-flowing capillaries between conditions.

Previous evidence indicates that muscle capillaries increase in diameter by  $\sim 0.5$ – $1.0$   $\mu\text{m}$  from their arteriolar to venular ends (Smaje et al., 1970). Although  $d_{cap}$  measurements herein were not normalized for the distance from arteriolar or venular ends, our  $d_{cap}$  assessment at random sites along the capillary length is not anticipated to introduce systematic errors. Moreover, capillary structural and hemodynamics analyses of the same microcirculatory fields within a given animal (and, in 47% of the cases, within the same capillary between CON and GLI conditions) likely minimized the potential for biases (including spatial vascular/metabolic heterogeneity, and heterogeneous  $f_{RBC}$ ,  $V_{RBC}$  and  $Hct_{cap}$  distributions) to be expressed in the present results. The lack of changes in  $d_{cap}$  in the face of reduced  $f_{RBC}$  and  $V_{RBC}$  with GLI (Figure 2) is consistent with upstream arteriolar regulation of skeletal muscle blood flow as mentioned above (Joyner & Casey, 2015; Kindig & Poole, 2001; Laughlin et al., 2012; Segal, 2005).

## 4.5 | Summary and conclusions

Local inhibition of  $K_{ATP}$  channels with GLI did not reduce the proportion of capillaries supporting continuous RBC flow or  $Hct_{cap}$  in the resting rat spinotrapezius muscle. These data are indicative of preserved muscle  $O_2$  diffusing capacity ( $DO_{2m}$ ) with GLI. In contrast, GLI lowered both  $f_{RBC}$  and  $V_{RBC}$  thus impairing perfusive microvascular  $O_2$  transport ( $Q_m$ ) and lengthening RBC capillary transit times, respectively. Considering the interdependence between diffusive and perfusive  $O_2$  conductances (i.e., % $O_2$  extraction determined largely by the local  $DO_{2m}/Q_m$ ; vide Eq. 2 above) (Roca et al., 1992), such GLI-induced alterations in capillary hemodynamics are expected to elevate muscle fractional  $O_2$  extraction to sustain a given metabolic rate. Taken together, the current results suggest that  $K_{ATP}$  channels regulate

capillary hemodynamics (and, therefore, microvascular gas exchange) in resting skeletal muscle.

## ACKNOWLEDGMENTS

We thank Ms. K. Sue Hageman for expert technical assistance and Dr. Clark T. Holdsworth for helpful discussion and guidance regarding glibenclamide superfusion in this study.

## DISCLOSURE

No conflicts of interest, financial or otherwise, are declared by the authors.

## AUTHOR CONTRIBUTIONS

DMH, TIM, and DCP conceived and designed research; DMH, AT, JCC, and TDC performed experiments; DMH analyzed data; DMH, TIM, and DCP interpreted results of experiments; DMH prepared figures and drafted manuscript; DMH, AT, JCC, TDC, TIM, and DCP edited and revised manuscript; DMH, AT, JCC, TDC, TIM, and DCP approved final version of the manuscript.

## ORCID

Daniel M. Hirai  <https://orcid.org/0000-0002-7861-637X>

## REFERENCES

- Altman, P., & Dittmer, D. (1974). *Biology data book*, 2nd ed. Federation of American Societies for Experimental Biology.
- Bailey, J. K., Kindig, C. A., Behnke, B. J., Musch, T. I., Schmid-Schoenbein, G. W., & Poole, D. C. (2000). Spinotrapezius muscle microcirculatory function: Effects of surgical exteriorization. *American Journal of Physiology. Heart and Circulatory Physiology*, 279, H3131–3137. <https://doi.org/10.1152/ajpheart.2000.279.6.H3131>.
- Bank, A. J., Sih, R., Mullen, K., Osayamwen, M., & Lee, P. C. (2000). Vascular ATP-dependent potassium channels, nitric oxide, and human forearm reactive hyperemia. *Cardiovascular Drugs and Therapy*, 14, 23–29. <https://doi.org/10.1023/a:1007835003493>.
- Berg, B. R., & Sarelius, I. H. (1996). Erythrocyte flux in capillary networks during maturation: Implications for oxygen delivery. *American Journal of Physiology*, 271, H2263–2273. <https://doi.org/10.1152/ajpheart.1996.271.6.H2263>.
- Cohen, K. D., Berg, B. R., & Sarelius, I. H. (2000). Remote arteriolar dilations in response to muscle contraction under capillaries. *American Journal of Physiology. Heart and Circulatory Physiology*, 278, H1916–1923. <https://doi.org/10.1152/ajpheart.2000.278.6.H1916>.
- Cohen, K. D., & Sarelius, I. H. (2002). Muscle contraction under capillaries in hamster muscle induces arteriolar dilatation via  $K_{ATP}$  channels and nitric oxide. *Journal of Physiology*, 539, 547–555. <https://doi.org/10.1113/jphysiol.2001.013388>.
- Colburn, T. D., Holdsworth, C. T., Craig, J. C., Hirai, D. M., Montgomery, S., Poole, D. C., Musch, T. I., & Kenney, M. J. (2020). ATP-sensitive  $K^+$  channel inhibition in rats decreases kidney and skeletal muscle blood flow without increasing sympathetic nerve discharge. *Respiratory Physiology & Neurobiology*, 278, 103444. <https://doi.org/10.1016/j.resp.2020.103444>.

- Colburn, T. D., Weber, R. E., Hageman, K. S., Caldwell, J. T., Schulze, K. M., Ade, C. J., Behnke, B. J., Poole, D. C., & Musch, T. I. (2020). Vascular ATP-sensitive K<sup>+</sup> channels support maximal aerobic capacity and critical speed via convective and diffusive O<sub>2</sub> transport. *The Journal of Physiology*, *598*, 4843–4858. <https://doi.org/10.1113/JIP280232>.
- Copp, S. W., Ferreira, L. F., Herspring, K. F., Musch, T. I., & Poole, D. C. (2009). The effects of aging on capillary hemodynamics in contracting rat spinotrapezius muscle. *Microvascular Research*, *77*, 113–119. <https://doi.org/10.1016/j.mvr.2008.11.001>.
- Delp, M. D., & Duan, C. (1996). Composition and size of type I, IIA, IID/X, and IIB fibers and citrate synthase activity of rat muscle. *Journal of Applied Physiology*, *80*, 261–270.
- Desjardins, C., & Duling, B. R. (1990). Heparinase treatment suggests a role for the endothelial cell glycocalyx in regulation of capillary hematocrit. *American Journal of Physiology*, *258*, H647–654. <https://doi.org/10.1152/ajpheart.1990.258.3.H647>.
- Duncker, D. J., Oei, H. H., Hu, F., Stubenitsky, R., & Verdouw, P. D. (2001). Role of K<sup>+</sup><sub>ATP</sub> channels in regulation of systemic, pulmonary, and coronary vasomotor tone in exercising swine. *American Journal of Physiology. Heart and Circulatory Physiology*, *280*, H22–33. <https://doi.org/10.1152/ajpheart.2001.280.1.H22>.
- Ellsworth, M. L., Ellis, C. G., Goldman, D., Stephenson, A. H., Dietrich, H. H., & Sprague, R. S. (2009). Erythrocytes: oxygen sensors and modulators of vascular tone. *Physiology*, *24*, 107–116. <https://doi.org/10.1152/physiol.00038.2008>.
- Farouque, H. M. O., & Meredith, I. T. (2003a). Effects of inhibition of ATP-sensitive potassium channels on metabolic vasodilation in the human forearm. *Clinical Science*, *104*, 39–46.
- Farouque, H. M. O., & Meredith, I. T. (2003b). Relative contribution of vasodilator prostanoids, NO, and K<sub>ATP</sub> channels to human forearm metabolic vasodilation. *American Journal of Physiology. Heart and Circulatory Physiology*, *284*, H2405–2411. <https://doi.org/10.1152/ajpheart.00879.2002>.
- Federspiel, W. J., & Popel, A. S. (1986). A theoretical analysis of the effect of the particulate nature of blood on oxygen release in capillaries. *Microvascular Research*, *32*, 164–189.
- Forkman, J. (2009). Estimator and tests for common coefficients of variation in normal distributions. *Communications in Statistics—Theory and Methods*, *38*, 233–251.
- Foster, M. N., & Coetzee, W. A. (2016). K<sub>ATP</sub> channels in the cardiovascular system. *Physiological Reviews*, *96*, 177–252. <https://doi.org/10.1152/physrev.00003.2015>.
- Gray, S. D. (1973). Rat spinotrapezius muscle preparation for microscopic observation of the terminal vascular bed. *Microvascular Research*, *5*, 395–400.
- Gray, S. D. (1984). Morphometric analysis of skeletal muscle capillaries in early spontaneous hypertension. *Microvascular Research*, *27*, 39–50. [https://doi.org/10.1016/0026-2862\(84\)90040-2](https://doi.org/10.1016/0026-2862(84)90040-2).
- Groebe, K., & Thews, G. (1990). Calculated intra- and extracellular PO<sub>2</sub> gradients in heavily working red muscle. *American Journal of Physiology*, *259*, H84–92.
- Hammer, L. W., Ligon, A. L., & Hester, R. L. (2001). Differential inhibition of functional dilation of small arterioles by indomethacin and glibenclamide. *Hypertension*, *37*, 599–603. <https://doi.org/10.1161/01.hyp.37.2.599>.
- Hirai, D. M., Colburn, T. D., Craig, J. C., Hotta, K., Kano, Y., Musch, T. I., & Poole, D. C. (2019). Skeletal muscle interstitial O<sub>2</sub> pressures: bridging the gap between the capillary and myocyte. *Microcirculation*, *26*, e12497. <https://doi.org/10.1111/micc.12497>.
- Hodnett, B. L., Xiang, L., Dearman, J. A., Carter, C. B., & Hester, R. L. (2008). K<sub>ATP</sub>-mediated vasodilation is impaired in obese Zucker rats. *Microcirculation*, *15*, 485–494. <https://doi.org/10.1080/10739680801942240>.
- Hogan, M. C., Arthur, P. G., Bebout, D. E., Hochachka, P. W., & Wagner, P. D. (1992). Role of O<sub>2</sub> in regulating tissue respiration in dog muscle working in situ. *Journal of Applied Physiology*, *73*, 728–736.
- Holdsworth, C. T., Copp, S. W., Ferguson, S. K., Sims, G. E., Poole, D. C., & Musch, T. I. (2015). Acute inhibition of ATP-sensitive K<sup>+</sup> channels impairs skeletal muscle vascular control in rats during treadmill exercise. *American Journal of Physiology. Heart and Circulatory Physiology*, *308*, H1434–1442. <https://doi.org/10.1152/ajpheart.00772.2014>.
- Holdsworth, C. T., Ferguson, S. K., Colburn, T. D., Fees, A. J., Craig, J. C., Hirai, D. M., Poole, D. C., & Musch, T. I. (2017). Vascular K<sub>ATP</sub> channels mitigate severe muscle O<sub>2</sub> delivery-utilization mismatch during contractions in chronic heart failure rats. *Respiratory Physiology & Neurobiology*, *238*, 33–40. <https://doi.org/10.1016/j.resp.2017.01.009>.
- Holdsworth, C. T., Ferguson, S. K., Poole, D. C., & Musch, T. I. (2016). Modulation of rat skeletal muscle microvascular O<sub>2</sub> pressure via K<sub>ATP</sub> channel inhibition following the onset of contractions. *Respiratory Physiology & Neurobiology*, *222*, 48–54. <https://doi.org/10.1016/j.resp.2015.11.012>.
- Jackson, W. F. (1993). Arteriolar tone is determined by activity of ATP-sensitive potassium channels. *American Journal of Physiology*, *265*, H1797–1803. <https://doi.org/10.1152/ajpheart.1993.265.5.H1797>.
- Jackson, W. F. (2017). Potassium channels in regulation of vascular smooth muscle contraction and growth. *Advances in Pharmacology*, *78*, 89–144. <https://doi.org/10.1016/bs.apha.2016.07.001>.
- Jiang, B., Wu, L., & Wang, R. (2007). Sulphonylureas induced vasorelaxation of mouse arteries. *European Journal of Pharmacology*, *577*, 124–128. <https://doi.org/10.1016/j.ejphar.2007.09.007>.
- Joyner, M. J., & Casey, D. P. (2015). Regulation of increased blood flow (hyperemia) to muscles during exercise: A hierarchy of competing physiological needs. *Physiological Reviews*, *95*, 549–601. <https://doi.org/10.1152/physrev.00035.2013>.
- Kano, Y., Padilla, D. J., Behnke, B. J., Hageman, K. S., Musch, T. I., & Poole, D. C. (2005). Effects of eccentric exercise on microcirculation and microvascular oxygen pressures in rat spinotrapezius muscle. *Journal of Applied Physiology*, *99*, 1516–1522. <https://doi.org/10.1152/jappphysiol.00069.2005>.
- Keller, D. M., Ogoh, S., Greene, S., Olivencia-Yurvati, A., & Raven, P. B. (2004). Inhibition of K<sub>ATP</sub> channel activity augments baroreflex-mediated vasoconstriction in exercising human skeletal muscle. *Journal of Physiology*, *561*, 273–282. <https://doi.org/10.1113/jphysiol.2004.071993>.
- Kindig, C. A., Musch, T. I., Basaraba, R. J., & Poole, D. C. (1999). Impaired capillary hemodynamics in skeletal muscle of rats in chronic heart failure. *Journal of Applied Physiology*, *87*, 652–660.
- Kindig, C. A., & Poole, D. C. (2001). Sarcomere length-induced alterations of capillary hemodynamics in rat spinotrapezius muscle: vasoactive vs passive control. *Microvascular Research*, *61*, 64–74. <https://doi.org/10.1006/mvre.2000.2284>.
- Kindig, C. A., Richardson, T. E., & Poole, D. C. (2002). Skeletal muscle capillary hemodynamics from rest to contractions: implications for

- oxygen transfer. *Journal of Applied Physiology*, 92, 2513–2520. <https://doi.org/10.1152/jappphysiol.01222.2001>.
- Kindig, C. A., Sexton, W. L., Fedde, M. R., & Poole, D. C. (1998). Skeletal muscle microcirculatory structure and hemodynamics in diabetes. *Respiration Physiology*, 111, 163–175.
- Laughlin, M. H., Davis, M. J., Secher, N. H., van Lieshout, J. J., Arce-Esquivel, A. A., Simmons, G. H., Bender, S. B., Padilla, J., Bache, R. J., Merkus, D., & Duncker, D. J. (2012). Peripheral circulation. *Comprehensive Physiology*, 2, 321–447. <https://doi.org/10.1002/cphy.c100048>.
- Leek, B. T., Mudaliar, S. R., Henry, R., Mathieu-Costello, O., & Richardson, R. S. (2001). Effect of acute exercise on citrate synthase activity in untrained and trained human skeletal muscle. *American Journal of Physiology: Regulatory, Integrative and Comparative Physiology*, 280, R441–447.
- Lu, S., Xiang, L., Clemmer, J. S., Gowdey, A. R., Mittwede, P. N., & Hester, R. L. (2013). Impaired vascular  $K_{ATP}$  function attenuates exercise capacity in obese Zucker rats. *Microcirculation*, 20, 662–669. <https://doi.org/10.1111/micc.12065>.
- Mazzoni, M. C., Skalak, T. C., & Schmid-Schönbein, G. W. (1990). Effects of skeletal muscle fiber deformation on lymphatic volumes. *American Journal of Physiology*, 259, H1860–1868. <https://doi.org/10.1152/ajpheart.1990.259.6.H1860>.
- Mele, A., Calzolaro, S., Cannone, G., Cetrone, M., Conte, D., & Tricarico, D. (2014). Database search of spontaneous reports and pharmacological investigations on the sulfonylureas and glinides-induced atrophy in skeletal muscle. *Pharmacology Research & Perspectives*, 2, e00028. <https://doi.org/10.1002/prp2.28>.
- Montvida, O., Shaw, J., Atherton, J. J., Stringer, F., & Paul, S. K. (2018). Long-term trends in antidiabetes drug usage in the U.S.: Real-world evidence in patients newly diagnosed with type 2 diabetes. *Diabetes Care*, 41, 69–78. <https://doi.org/10.2337/dc17-1414>.
- Murrant, C. L., & Sarelius, I. H. (2002). Multiple dilator pathways in skeletal muscle contraction-induced arteriolar dilations. *American Journal of Physiology: Regulatory, Integrative and Comparative Physiology*, 282, R969–978. <https://doi.org/10.1152/ajprgu.00405.2001>.
- Padilla, D. J., McDonough, P., Behnke, B. J., Kano, Y., Hageman, K. S., Musch, T. I., & Poole, D. C. (2006). Effects of Type II diabetes on capillary hemodynamics in skeletal muscle. *American Journal of Physiology: Heart and Circulatory Physiology*, 291, H2439–2444. <https://doi.org/10.1152/ajpheart.00290.2006>.
- Poole, D. C., Copp, S. W., Hirai, D. M., & Musch, T. I. (2011). Dynamics of muscle microcirculatory and blood-myocyte  $O_2$  flux during contractions. *Acta Physiologica*, 202, 293–310. <https://doi.org/10.1111/j.1748-1716.2010.02246.x>.
- Poole, D. C. (2019). Edward F. Adolph distinguished lecture. Contemporary model of muscle microcirculation. *Journal of Applied Physiology*, 127, 1012–1033. <https://doi.org/10.1152/jappphysiol.00013.2019>.
- Poole, D. C., Musch, T. I., & Kindig, C. A. (1997). In vivo microvascular structural and functional consequences of muscle length changes. *American Journal of Physiology*, 272, H2107–2114. <https://doi.org/10.1152/ajpheart.1997.272.5.H2107>.
- Pries, A. R., Ley, K., & Gaehtgens, P. (1986). Generalization of the Fahraeus principle for microvessel networks. *American Journal of Physiology*, 251, H1324–1332. <https://doi.org/10.1152/ajpheart.1986.251.6.H1324>.
- Richardson, T. E., Kindig, C. A., Musch, T. I., & Poole, D. C. (2003). Effects of chronic heart failure on skeletal muscle capillary hemodynamics at rest and during contractions. *Journal of Applied Physiology*, 95, 1055–1062. <https://doi.org/10.1152/jappphysiol.0100308.2003>.
- Roca, J., Agusti, A. G., Alonso, A., Poole, D. C., Viegas, C., Barbera, J. A., Rodriguez-Roisin, R., Ferrer, A., & Wagner, P. D. (1992). Effects of training on muscle  $O_2$  transport at  $VO_{2max}$ . *Journal of Applied Physiology*, 73, 1067–1076.
- Rocha, M. P., Campos, M. O., Mattos, J. D., Mansur, D. E., Rocha, H. N. M., Secher, N. H., Nóbrega, A. C. L., & Fernandes, I. A. (2020).  $K_{ATP}$  channels modulate cerebral blood flow and oxygen delivery during isocapnic hypoxia in humans. *Journal of Physiology*, 598, 3343–3356. <https://doi.org/10.1113/JP279751>.
- Russell, J. A., Kindig, C. A., Behnke, B. J., Poole, D. C., & Musch, T. I. (2003). Effects of aging on capillary geometry and hemodynamics in rat spinotrapezius muscle. *American Journal of Physiology: Heart and Circulatory Physiology*, 285, H251–258. <https://doi.org/10.1152/ajpheart.01086.2002>.
- Saito, Y., McKay, M., Eraslan, A., & Hester, R. L. (1996). Functional hyperemia in striated muscle is reduced following blockade of ATP-sensitive potassium channels. *American Journal of Physiology*, 270, H1649–1654. <https://doi.org/10.1152/ajpheart.1996.270.5.H1649>.
- Sarelius, I. H. (1986). Cell flow path influences transit time through striated muscle capillaries. *American Journal of Physiology*, 250, H899–907. <https://doi.org/10.1152/ajpheart.1986.250.6.H899>.
- Sarelius, I. H., & Duling, B. R. (1982). Direct measurement of microvesSEL hematocrit, red cell flux, velocity, and transit time. *American Journal of Physiology*, 243, H1018–1026. <https://doi.org/10.1152/ajpheart.1982.243.6.H1018>.
- Secomb, T. W., Hsu, R., & Pries, A. R. (1998). A model for red blood cell motion in glycocalyx-lined capillaries. *American Journal of Physiology*, 274, H1016–1022. <https://doi.org/10.1152/ajpheart.1998.274.3.H1016>.
- Segal, S. S. (2005). Regulation of blood flow in the microcirculation. *Microcirculation*, 12, 33–45. <https://doi.org/10.1080/10739680590895028>.
- Smaje, L., Zweifach, B. W., & Intaglietta, M. (1970). Micropressures and capillary filtration coefficients in single vessels of the cremaster muscle of the rat. *Microvascular Research*, 2, 96–110. [https://doi.org/10.1016/0026-2862\(70\)90055-5](https://doi.org/10.1016/0026-2862(70)90055-5).
- Thomas, G. D., Hansen, J., & Victor, R. G. (1997). ATP-sensitive potassium channels mediate contraction-induced attenuation of sympathetic vasoconstriction in rat skeletal muscle. *Journal of Clinical Investigation*, 99, 2602–2609. <https://doi.org/10.1172/JCI119448>.
- Tricarico, D., Mele, A., Lundquist, A. L., Desai, R. R., George, A. L., & Conte, C. D. (2006). Hybrid assemblies of ATP-sensitive  $K^+$  channels determine their muscle-type-dependent biophysical and pharmacological properties. *Proceedings of the National Academy of Sciences*, 103, 1118–1123. <https://doi.org/10.1073/pnas.0505974103>.
- Tykocki, N. R., Boerman, E. M., & Jackson, W. F. (2017). Smooth muscle ion channels and regulation of vascular tone in resistance arteries and arterioles. *Comprehensive Physiology*, 7, 485–581. <https://doi.org/10.1002/cphy.c160011>.
- Vanelli, G., & Hussain, S. N. (1994). Effects of potassium channel blockers on basal vascular tone and reactive hyperemia of canine diaphragm. *American Journal of Physiology*, 266, H43–51. <https://doi.org/10.1152/ajpheart.1994.266.1.H43>.
- Welsh, D. G., & Segal, S. S. (1996). Muscle length directs sympathetic nerve activity and vasomotor tone in resistance vessels of

- hamster retractor. *Circulation Research*, 79, 551–559. <https://doi.org/10.1161/01.res.79.3.551>.
- Wilson, D. F., Erecińska, M., Drown, C., & Silver, I. A. (1977). Effect of oxygen tension on cellular energetics. *American Journal of Physiology*, 233, C135–140.
- Xiang, L., & Hester, R. L. (2009). Adipocyte-derived factor reduces vasodilatory capability in *ob/ob*- mice. *American Journal of Physiology. Heart and Circulatory Physiology*, 297, H689–695. <https://doi.org/10.1152/ajpheart.01327.2008>.
- Zar, J. H. (1984). *Biostatistical analysis*, 2nd ed. Prentice-Hall.

**How to cite this article:** Hirai DM, Tabuchi A, Craig JC, Colburn TD, Musch TI, Poole DC. Regulation of capillary hemodynamics by  $K_{ATP}$  channels in resting skeletal muscle. *Physiol Rep*. 2021;9:e14803. <https://doi.org/10.14814/phy2.14803>